BMC Neuroscience

BioMed Central

Research article

Growth Cone Pathfinding: a competition between deterministic and stochastic events

Susan M Maskery[1], Helen M Buettner[1,2] and Troy Shinbrot*[2]

Address: [1]Department of Chemical and Biochemical Engineering, Rutgers University, 98 Brett Road, Piscataway, NJ, 08854, USA and [2]Department of Biomedical Engineering, Rutgers University, 617 Bowser Road, Piscataway, NJ, 08854, USA

Email: Susan M Maskery - smaskery@soemail.rutgers.edu; Helen M Buettner - buettner@rci.rutgers.edu; Troy Shinbrot* - shinbrot@soemail.rutgers.edu

* Corresponding author

Published: 08 July 2004

BMC Neuroscience 2004, **5**:22 doi:10.1186/1471-2202-5-22

Received: 25 March 2004
Accepted: 08 July 2004

This article is available from: http://www.biomedcentral.com/1471-2202/5/22

Abstract

Background: Growth cone migratory patterns show evidence of both deterministic and stochastic search modes.

Results: We quantitatively examine how these two different migration modes affect the growth cone's pathfinding response, by simulating growth cone contact with a repulsive cue and measuring the resultant turn angle. We develop a dimensionless number, we call the determinism ratio Ψ, to define the ratio of deterministic to stochastic influences driving the growth cone's migration in response to an external guidance cue. We find that the growth cone can exhibit three distinct types of turning behaviors depending on the magnitude of Ψ.

Conclusions: We conclude, within the context of these *in silico* studies, that only when deterministic and stochastic migration factors are in balance (i.e. $\Psi \sim 1$) can the growth cone respond constructively to guidance cues.

Background

Understanding how individual neurons are so reliably guided to their targets during development may be considered a crucial first step to developing successful therapies for neuronal injury. Previous work has focused on understanding how the growth cone – a sensory motile structure at the end of a growing neurite – navigates through a complex extracellular environment [for review [1-4]: see also [5-12]]. It has been shown that, at a minimum multiple guidance cues whose expression patterns are controlled both temporally and spatially, are necessary for neurons to reach their targets [13-20]. *In vivo* experiments have shown that during development, the growth cone's migration pattern undergoes a transition near major pathfinding decision regions [21-24]. When not in a decision region, growth cone migration is relatively constant. By contrast, when in a decision region, forward migration frequently stalls and the growth cone becomes morphologically complex. This type of behavior is suggestive of at least two migratory states, one purposeful and deterministic, and a second erratic and stochastic.

We report here simulation results that show that growth cone migration does indeed transition between a deterministic state (where growth is characterized by smooth forward motion without abrupt directional changes) and a stochastic state (where growth is characterized by frequent pauses and sudden abrupt directional changes). We find that *only at the transition between stochastically-dominated and deterministically-dominated motion, is guidance by traditionally tested environmental factors* [25,26]*possible*. Based on these computational results, that we develop

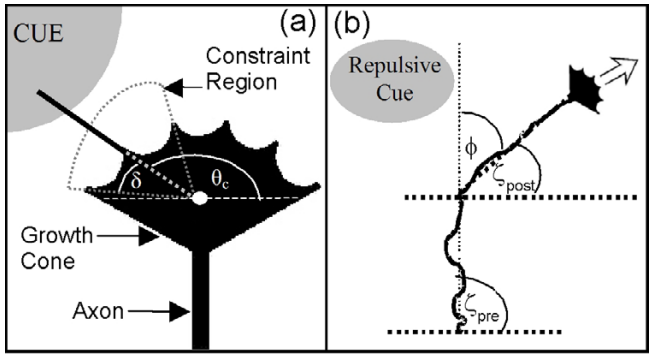

Figure 1
Illustrations of Important Simulation Parameters and Quantities Measured. (a) Sketch of constraint region, an angular region of size 2δ centered at the contacting filopodium's initiation angle θ_c, which is created by filopodial contact with a guidance cue. The growth cone cannot migrate into the constraint region. (b) A repulsive cue migration sequence where the growth cone migrates with a pre-contact trajectory angle ζ_{pre} until it makes filopodial contact with a repulsive cue. The turn angle ϕ is calculated from the difference between the pre-contact trajectory angle ζ_{pre} and the post-contact trajectory angle ζ_{post}.

next, we conjecture that this state, balanced on the edge of stability, developed as an effective strategy to produce accurate searching, targeting, and pathfinding.

Results

Simulation of growth cone migration and guidance

Various random walk models capable of capturing crucial stochastic [5,27,28] and deterministic [5,27,29] aspects of growth cone movement have been adapted to simulate growth cone migration [9,30-32]. We use the simplest of these models. Migration is simulated in 2-dimensions, and correspondingly two equations are used. One equation models migration in the direction of axonal outgrowth (Δy_{ct}); the second models migration in the orthogonal direction (Δx_{ct}) [30]. Explicitly,

$$\Delta x_{ct} = e_{xt} \quad (1)$$

$$\Delta y_{ct} = e_{yt} + \Delta y_{avg} \quad (2)$$

where Δx_{ct} and Δy_{ct} equal the change in the growth cone centroid coordinates, x_c and y_c respectively, over a time interval τ. The e_{xt} and e_{yt} terms are drawn from independent and normal random distributions with zero means and constant standard deviations $\sigma_{dx}\sqrt{\tau}$ and $\sigma_{dy}\sqrt{\tau}$ respectively. These deviations are explicitly normalized with respect to time step τ [33] to generate behaviors whose statistics do not depend on the numerical choice of the simulation time step. Stochastic migration distances will grow with $\sqrt{\tau}$, just as they would by a random diffusive process.

To model the effect of a repulsive cue, we block migration in the direction of contact θ_c plus or minus a constraint parameter δ (i.e. $\theta_c \pm \delta$). As shown in Fig. 1(a), θ_c sets the direction of filopodium-cue contact and is measured relative to the positive x-axis of the growth cone, and δ sets the size of the constraint region, which is in turn representative of the strength of the cue. A large δ characterizes a strongly repulsive cue, a small δ characterizes a weakly repulsive cue.

We measure the inhibitory impact of the constraint region $\theta_c \pm \delta$ on a migrating growth cone by calculating the resulting turn angle ϕ in a manner similar to turn assays developed *in vitro* [26,34]. As illustrated in Fig. 1(b), ζ_{pre} is the migration trajectory angle before contact with a guidance cue, and ζ_{post} is the migration trajectory angle after contact with a guidance cue. The turn angle ϕ is defined as the difference between pre-contact and post-contact trajectory angles:

$$\phi = \zeta_{pre} - \zeta_{post.} \quad (3)$$

Migratory behavior resultant from contact with a discrete repulsive cue

To summarize, in our simulations contact with a repulsive cue prevents future migration toward the cue, i.e. in the direction $\theta_c \pm \delta$, and we quantify the resulting change in migration direction in terms of the turn angle ϕ. The expected value of the turn angle ϕ as a function of the contact angle θ_c, the constraint size δ, and the characteristic time τ, is in turn calculated from the determinism ratio $\Psi(\theta_c, \delta, \tau)$ (please see our methods section for a detailed derivation of Ψ). The determinism ratio Ψ is dimensionless, and captures the ratio of mean deterministic migration to mean stochastic migration.

Algorithmically, we evaluate the actual dependence of the turn angle ϕ on the constraint region $\theta_c \pm \delta$ – i.e. how a growth cone can be expected to respond to a repulsive cue in its environment – by varying the location of the constraint region in 5° intervals from θ_c = 95° to 150°, and the size of the constraint region, also in 5° intervals, from δ = 5° to 20°. We then calculate the determinism ratio $\Psi(\theta_c, \delta, \tau)$ as described in our methods section for all 48 constraint regions $\theta_c \pm \delta$, and for 18 characteristic times τ. Characteristic times ranged in value over five orders of magnitude from 10^{-6} s to 500 s.

In Fig. 2 we plot the resultant turn angle ϕ as a function of the determinism ratio Ψ for all 864 combinations of θ_c,δ,

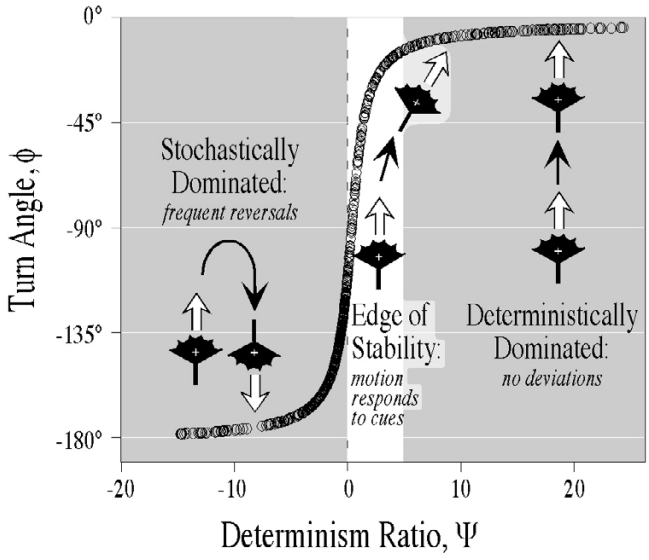

Figure 2
Turn Angle ϕ as a Function of Determinism Ratio Ψ. The determinism ratio Ψ is a dimensionless number calculated from θ_c, δ, and τ. The turn angle ϕ is plotted as a function of Ψ. hree states emerge when the turn angle ϕ is plotted as a function of the determinism ratio Ψ. At ϕ = -180° random migration dominates. The growth cone always collapses. The second state is a transition region where deterministic and stochastic motions are balanced. This region occurs over a narrow region where random migration and deterministic migration are comparable. At ϕ = 0° deterministic migration dominates. Growth cone migration is unaffected by size or placement of the constraint region.

and τ. From this figure, it is evident that all computational data fall onto a single continuous curve. When Ψ is negative, migration is dominated by the stochastic terms in Eq's. (1)-(2), and the turn angle is always significant and negative. Such a state exhibits essentially no net forward motion, which we interpret as leading to growth cone collapse. The turn angle ϕ is often close to -180° resulting in the U-turn like motion depicted in the lower-left inset to Fig. 2. On the other hand, when Ψ ~1, stochastic and deterministic motion are comparable, and the curve is in a critical region where the turn angle is sensitive to a guidance cue. This turn behavior, in which the growth cone turns away from the repulsive cue but does not collapse, is depicted in the central inset to Fig. 2. The upper end of the curve shown in Fig. 2 corresponds to an expected turn angle of zero. In this case, the deterministic term $\Delta y_{avg}\tau$ in Eq's. (2), (9) dominates migration, and as a consequence, the growth cone does not alter its migrational direction in response to a repulsive cue. This type of behavior is sketched in the upper right inset to Fig. 2. In summary, based upon our simulation data we conclude that the growth cone turn angle is *insensitive* to repulsive cues for negative Ψ (in which case the growth cone wanders energetically) or for large Ψ (in which case the growth cone moves forward nearly unaffected by cue contact). *Only in a narrow critical region between these extremes, where stochastic growth and deterministic growth are balanced, is directed migration possible.*

To further explore the influence of stochastic and deterministic factors on the expected turn angle ϕ, in Fig. 3 we analyze turn behavior at different values of characteristic time τ for 56 distinct constraint regions $\theta_c \pm \delta$. The location of the constraint region is varied in 5° intervals from θ_c = 95° to 160°, and the size of the constraint region is varied in 10° intervals from δ = 10° to 40°. In Fig. 3(a) the turn angle ϕ is plotted as a function of the determinism ratio Ψ, and in Fig. 3(b) the turn angle ϕ is plotted against the contact angle θ_c. Each graph in Fig. 3(b) contains four curves that correspond to four constraint sizes δ. All data are replicated for the three different choices of τ indicated.

Examining Fig. 3(a) first, we see that for a short characteristic time (τ = 0.001 s) all turn angles are very large and as we have suggested, this may be interpreted as leading to collapse of the growth cone. With or without this interpretation, it is clear that rapid exploratory motion here swamps any purposeful forward growth. At τ = 10 s, many constraint regions result in turning behavior that is within the critical region of Fig. 2 where guided outgrowth without collapse is possible. In this case, both the size and placement of the constraint region are important in determining the turn angle, and *a complete range of turning behaviors*, from a complete change in direction to no turn at all, *are possible* at this characteristic time. At τ = 120 s, on the other hand, the majority of constraint regions result in no turn angle. A few constraint regions result in a determinism ratio Ψ that is at the edge of transition between essentially random migration and deterministic migration, however, the growth cone's sensitivity to guidance cues is profoundly suppressed.

Fig. 3(b) explicitly displays the effect of the contact angle on turning behavior. Experimentally, the angle of contact with a cue has been shown to be a determinant in the eventual growth cone turning response [25]. For example, perpendicular contact (in our system this would be a contact angle close to 90°) of a motor neuron with the repulsive surface of the posterior sclerotome results in a larger turn angle (i.e. branching behavior) than more oblique contact with the same cue [25].

As in Fig. 3(a), we see that in Fig. 3(b) a small characteristic time (τ = 0.001 s) results in large turn angles that are indicative of growth cone collapse. However, by τ = 10 s

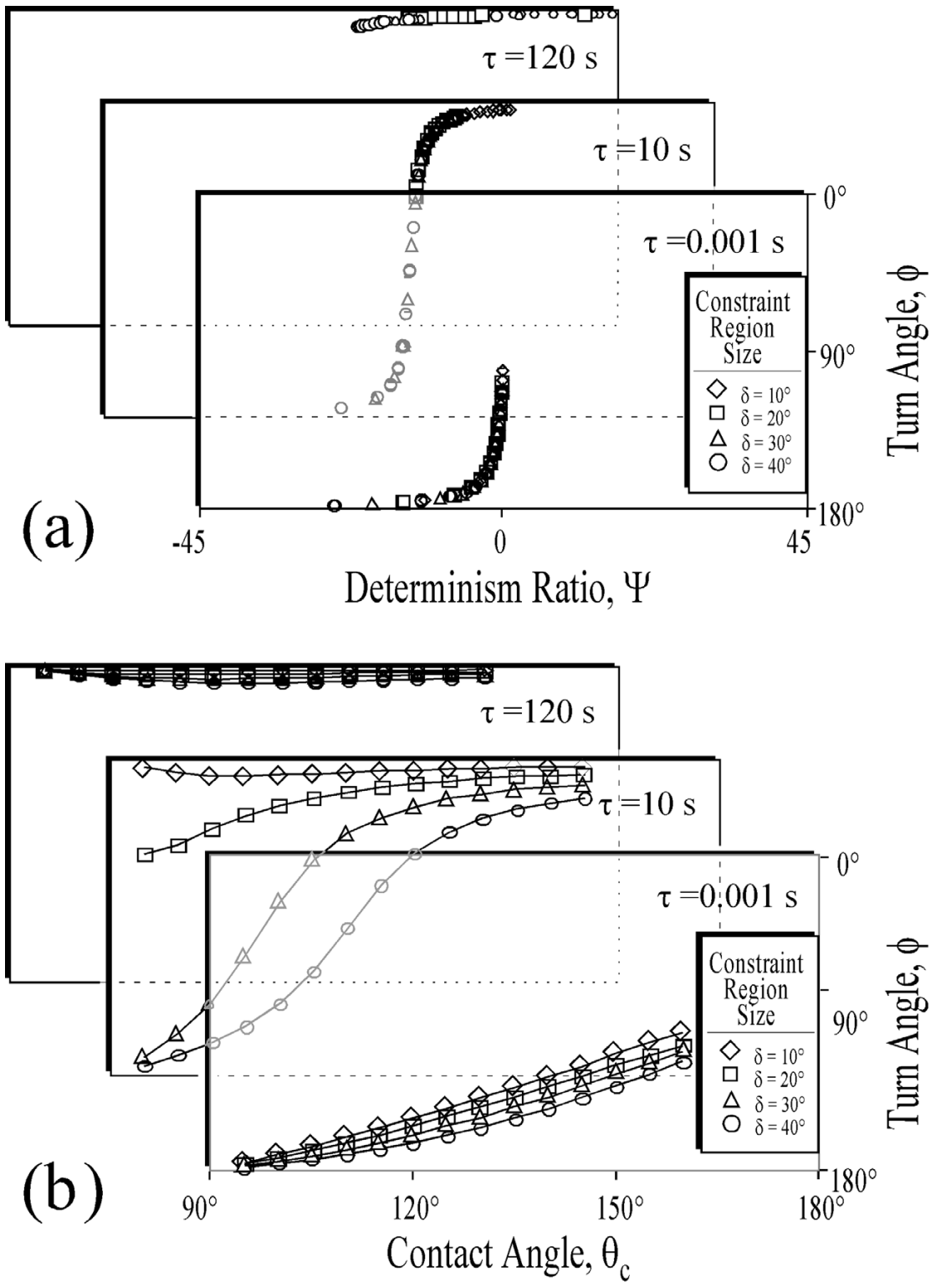

Figure 3

Turn Angle ϕ as a Function of Determinism Ratio Ψ (a) and as a Function of Contact Angle θ_c(b). The turn angle ϕ is plotted (a) as a function of the determinism ratio Ψ, and (b) as a function of the contact angle θ_c. As demonstrated in both (a) and (b), when $\tau << 1$ s, ϕ is always ~-180°. In contrast, when $\tau >> 1$ s, ϕ is always ~0°. Only at $\tau \sim 10$ s is guided migration possible through modulation of cue geometry and strength.

both contact angle and constraint size play much more significant roles in determining the turn angle response. For perpendicular contacts ($\theta_c \sim 90°$), strongly repulsive cues (i.e. those with large δ) produce complete reversal of the growth cone's direction. However, for more oblique contacts ($\theta_c \sim 135°$), a turn with continued forward outgrowth is possible. By a characteristic time $\tau \sim 120$ s, the angle of cue contact is no longer a determinant in turning behavior: the turn angle is essentially constant across all contact angles.

These results imply that the geometry of cue placement and the cue's repulsive strength can strongly control growth cone turning behavior when – and only when – the characteristic time τ is on the order of 10–90 s. Significantly, this is very close to the timescale associated with new filopodial [35] and lamellipodial [36,37] initiations in response to stimuli. The is a first suggestion of several that we discuss in the next section that supports the hypothesis that growth cone exploration time scales may be matched with forward migration speeds so as to support cue-responsive motion in which random exploration and forward motion are balanced near the edge of stability.

Discussion

We have gained insight into the mechanisms of growth cone guidance through the development and application of a quantitative model of growth cone guidance. We have reproduced, with a very simple model, stereotypical behavior seen *in vitro* [25,26,34,38]. Consistent with observed migratory behavior [23,39-42], our computational model predicts two primary migrational states based upon simple stochastic and deterministic behavioral dynamics. To calculate which migrational state the growth cone is within, we have defined a dimensionless measure, the determinism ratio Ψ, that captures the balance between stochastic and deterministic motions driving migration. Most significantly, we have found that the model parameter that determines whether stochastic or deterministic dynamics dominate migration, the characteristic time τ, is crucial to determining the growth cone's repulsive turn response. Importantly, the characteristic time τ is an indicator of endogenous growth cone migration dynamics, and is independent of exogenous factors such as the angle of cue contact and the cue's repulsive strength. At one extreme, when $\tau << 1$ s, stochastic motion dominates and significant changes in growth cone direction regularly occur independent of the size and location of the constraint region. At the opposite extreme, when $\tau >> 1$ s, deterministic motion dominates: no change in growth cone direction is possible, again independent of constraint region. Only between these two extremes is there a transition region where controlled changes in migration direction are possible.

From our analysis, we found that the balance between stochastic and deterministic dynamics, captured in our computational model for growth cone guidance via contact with a local repulsive cue, determines the growth cone's turn response. There is qualitative experimental evidence that suggests that multiple conversions between stochastic and deterministic growth states occur during development. For example, the growth cone undergoes significant structural remodeling in decision regions, developing a complex shape as it spreads outward and develops numerous filopodia [40]. Further, migration patterns become non-uniform, exhibiting frequent pauses or stalls [21,22,43]. When not in a decision region, growth cone morphology is characterized by a streamlined shape, and migration is far more uniform [21,22,43]. While not definitive, these data support the hypothesis that the growth cone can switch between stochastically and deterministically dominated growth, and that close to a decision region the growth cone transitions from one to another.

Without doubt, the growth cone is a finely tuned sensory structure capable of adapting to different environments. Its potential behaviors are much more nuanced and varied than the simplified model presented here can capture. However, our model does capture a broad range of turning behavior with a small number of biologically plausible parameters. Future work will focus on expanding the model to capture an increased range of neuronal pathfinding behaviors. For example, in the future we plan to explicitly account for axonal branching, an important mediator of neuronal pathfinding [44,45]. In addition to the situation of a lone pathfinder axon and its growth cone considered here, we would like to include interactive behavior between multiple axons, such as fasciculation, where populations of axons grow alongside one another. *In vitro* experiments have shown that the same cue can elicit either an attractive or a repulsive turn in response to the concentration of secondary messengers such as Ca^{2+} and cAMP within the growth cone [34,46], and we would like to account for this in future work. Additionally, consideration of fixed repulsive cues likely does not address the action of repulsive gradients. In response to contact with a repulsive gradient, it is likely that the growth cone would extend toward the steepest decrease in gradient strength [47].

The model of growth cone guidance by repulsion presented here is most appropriate for the sensing of local repulsive cues where the balance between stochastic and deterministic behaviors sets the turn response. Such a mechanism must exist in any guidance system containing both stochastic and deterministic growth [48-50]. We speculate the nervous system may well make use of such a

mechanism to regulate which neurons growth steadily and which may pause to explore their environment.

Conclusions

We have developed a model for growth cone guidance and migration that can be used to gain insight into how the balance between stochastic and deterministic behavioral dynamics can produce stereotypical growth cone behavior seen *in vivo* and *in vitro* [23,39-42]. To quantify this behavior, we have developed a dimensionless measure, the determinism ratio Ψ, to predict which migrational state the growth cone is within based upon the balance of stochastic to deterministic motions driving migration rates. When we the turn angle, ϕ, is plotted against Ψ, a stochastic dominated migration state and a deterministic dominated migration state are seen. It is in the transition between these two states that sustained growth cone guidance by a repulsive cue is possible and controllable.

Methods

Migration model parameter values

The model for growth cone migration has three parameters: Δy_{avg} the rate of growth cone migration in the y-axis (axonal) direction [5,30], and σ_{dx} and σ_{dy} the standard deviations of the growth cone migration rates in the x-axis (non-axonal) and y-axis (axonal) directions respectively. The value of Δy_{avg} is 0.019 μm/s. This value is calculated with non-axonal outgrowth removed as described in [5]. This migration rate is similar to previously published migration rates under similar culture conditions [30,51,52]. The standard deviation for growth cone migration in the axonal y-axis direction is σ_{dy} = 0.2 μm/s, the standard deviation for growth cone migration in the non-axonal x-axis direction is σ_{dx} = 0.1 μm/s. These parameter values are calculated from experimental measurements of dorsal root ganglion (DRG) growth cone migration on an uniform laminin surface as detailed in [31], elements of this protocol including DRG isolation, DRG culture conditions, and filming of DRG outgrowth have been described previously in [52].

Growth cone trajectory measurements

The migration trajectory angle ζ (Fig. 1(b)) is calculated from simulated growth cone centroid motion in relation to a fixed positive x-axis. Each trajectory angle is defined as the inverse tangent of the ratio of the time averaged values for simulation generated (x,y) centroid coordinates (<Δx> and <Δy> respectively) over a set time T, typically 30 minutes:

$$\zeta = \tan^{-1}(<\Delta y> / <\Delta x>) \quad (4)$$

Simulation of growth cone guidance by a discrete repulsive cue

As defined by Eq's. (1) and (2), growth cone migration is modeled as having explicit deterministic and stochastic components. It is important to emphasize that these two components make fundamentally different contributions to growth cone migration. Migration originating from deterministic motion is simply proportional to elapsed time, T: its integrated value is 0 in the x-direction and Δy_{avg}*T in the y-direction. By contrast, migration driven by stochastic motion grows as $c_1\sqrt{\tau}$ in the x-direction and $c_2\sqrt{\tau}$ in the y-direction, where c_1 and c_2 (see Eq's. (5) and (6)) are constants whose values depend on θ_c and δ. Consequently, even when stochastic growth is normalized with time step as we have done, the two components of motion *intrinsically and inevitably grow at different rates*. For large characteristic times, growth will be deterministically dominated, and for small characteristic times, growth will be stochastically dominated. The relative values of σ_{xt}, σ_{yt}, and Δy_{avg} in Eq's. (1)-(2) govern the timescale at which growth transitions from one regime to the other (discussed next), but regardless of these numerical values, a system driven both by stochastic and deterministic influences as in Eq's. (1)-(2) must exhibit distinct growth regimes for sufficiently small and large elapsed times.

To evaluate the transition time scale in the growth cone guidance problem, we have performed Monte Carlo simulations, in which we calculate migration in the axonal direction $\hat{y}$ and in the orthogonal non-axonal direction $\hat{x}$ by averaging stochastically-generated migration that we constrain such that $\tan^{-1}(\Delta y/\Delta x) \neq \theta_c \pm \delta$. Constrained migration is simulated for each θ_c, δ parameter combination for N = 3,600,0000 total simulation steps, the equivalent of 1 hour total time T simulated with time step τ equal to 0.001 s. Axonal directed migration constant, $c_2(\theta_c,\delta)$, and non-axonal directed migration constant, $c_1(\theta_c,\delta)$, are respectively defined as:

$$c_2(\theta_c,\delta) = \frac{\sum_{n=1}^{N} \Delta y(\theta_c,\delta)}{N\sqrt{\tau}} \quad (5)$$

$$c_1(\theta_c,\delta) = \frac{\sum_{n=1}^{N} \Delta x(\theta_c,\delta)}{N\sqrt{\tau}} \quad (6)$$

We repeat the evaluation of $c_1(\theta_c,\delta)$ and $c_2(\theta_c,\delta)$ 500 times for each θ_c,δ combination. The distances traveled in the x-

and y-directions used to calculate the post-contact trajectory angle are defined as:

$$\left\langle x(\theta_c,\delta)\right\rangle = c_1(\theta_c,\delta)\sqrt{\tau} \qquad (7)$$

$$\left\langle y(\theta_c,\delta)\right\rangle = c_2(\theta_c,\delta)\sqrt{\tau} + \Delta y_{avg}\tau \qquad (8)$$

Here we again see explicitly that the motion of a growth cone depends on the characteristic time τ. In the biological context, this time refers to the rapidity with which the growth cone explores its environment: if the growth cone wanders rapidly, τ will be small and Eq's. (7) and (8) will prescribe stochastically dominated motion, whereas if the growth cone moves steadily forward, τ will be large, and the deterministic term in Eq. (8) will dominate. The same results are obtained in our simulations, where the choice of τ dictates the character of growth.

It is important to clarify that in our simulation, the choice of normalization of the standard deviation of e_{xt} and e_{yt} in Eq's. (1) and (2) to $\sqrt{\tau}$ does not affect this intrinsic competition between stochastic and deterministic growth rates. The normalization used in Eq's. (1) and (2) merely allows us to set the parameters σ_{dx} and σ_{dy} independently of time step in a standard way – i.e. so that the *stochastic* part of a simulation with given values of these parameters will grow with the same rate for large or small τ. Irrespective of the choice of normalization, once parameters have been fixed, whether a neurite's motion is predominantly stochastic or deterministic depends on the relative time scales of its random and purposeful motions. We reiterate that this competition between stochastic and deterministic behaviors is a mathematically unavoidable consequence of the fact that stochastic processes grow with the square root of time, while a constant velocity drift grows linearly with time.

To examine how stochastic and deterministic factors compete, we define a determinism ratio, Ψ, to be the dimensionless ratio of the sum of mean deterministic migration $\Delta y_{avg}\tau$ and stochastic migration $c_2\sqrt{\tau}$ from Eq. (5) to mean stochastic migration, $c_1\sqrt{\tau}$, from Eq. (6). Thus for large and positive Ψ, growth is highly deterministic and for negative Ψ, growth is chiefly stochastic. Referring to Fig. 1(b), the post-contact trajectory angle ζ_{post} for a given characteristic time τ is calculated from the determinism ratio Ψ.

$$\left\langle \zeta_{post} \right\rangle = \tan^{-1}(\Psi) = \tan^{-1}\left(\frac{c_2(\theta_c,\delta)\sqrt{\tau} + \Delta y_{avg}\tau}{c_1(\theta_c,\delta)\sqrt{\tau}} \right) \qquad (9)$$

where we recall from Eq's. (5) and (6) that c_1, c_2, and hence $<\zeta_{post}>$, are functions of θ_c, δ, and τ. Finally, the expected value for the turn angle φ as a function θ_c, δ, and τ is calculated from the expected values of the pre-contact trajectory angle ζ_{pre} (initiated arbitrarily to 90°) and post-contact trajectory angle ζ_{post}:

$$<\phi(\theta_c,\delta,\tau)> = <\zeta_{pre}> - <\zeta_{post}(\theta_c,\delta,\tau)> \qquad (10)$$

Symbols and abbreviations

Ψ determinism ratio

τ characteristic time step

Δx_{ct} non-axonal outgrowth over time τ

Δy_{ct} axonal outgrowth over time τ

e_{xt} stochastic non-axonal outgrowth over time τ

e_{yt} stochastic axonal outgrowth over time τ

Δy_{avg} constant rate of axonal outgrowth

σ_{dx} non-axonal outgrowth standard deviation

σ_{dy} axonal outgrowth standard deviation

θ_c angle of filopodium-cue contact

δ constraint size parameter

ζ_{pre} pre-contact trajectory angle

ζ_{post} post-contact trajectory angle

φ turn angle

$\tan^{-1}$ inverse tangent function

c_1 stochastic motion constant arising from blocking non-axonal migration

c_2 stochastic motion constant arising from blocking axonal migration

N number of simulation time steps

T total simulation time (N*τ)

DRG dorsal root ganglion

Authors' contributions

SM designed and ran simulation experiments. SM, HB, and TS conceived of the study, and participated in its design and coordination. All authors read and approved the final manuscript.

Acknowledgements

This work was supported by grants from J&J, NJCHE, Rutgers SROA, and the Rutgers/UMDNJ Biotechnology Training Program. We thank Dr. Aquanette Burt for the use of her growth cone migration data.

References

1. Tessier-Lavigne M, Goodman CS: **The molecular biology of axon guidance.** *Science* 1996, **274:**1123-33.
2. Dodd J, Jessell TM: **Axon guidance and the patterning of neuronal projections in vertebrates.** *Science* 1988, **242:**692-9.
3. Mueller BK: **Growth cone guidance: first steps towards a deeper understanding.** *Annu Rev Neurosci* 1999, **22:**351-88.
4. Buettner HM: **Nerve growth dynamics. Quantitative models for nerve development and regeneration.** *Ann N Y Acad Sci* 1994, **745:**210-21.
5. Katz MJ, George EB, Gilbert LJ: **Axonal elongation as a stochastic walk.** *Cell Motil* 1984, **4:**351-70.
6. van Veen M, van Pelt J: **A model for outgrowth of branching neurites.** *Journal of Theoretical Biology* 1992, **159:**1-23.
7. Van Veen MP, Van Pelt J: **Neuritic growth rate described by modeling microtubule dynamics.** *Bulletin of Mathematical Biology* 1994, **56:**249-73.
8. Li GH, Qin CD, Li MH: **On the mechanisms of growth cone locomotion: modeling and computer simulation.** *J Theor Biol* 1994, **169:**355-62.
9. Buettner HM, Pittman RN, Ivins JK: **A model of neurite extension across regions of nonpermissive substrate: simulations based on experimental measurement of growth cone motility and filopodial dynamics.** *Dev Biol* 1994, **163:**407-22.
10. Goodhill GJ, Urbach JS: **Theoretical analysis of gradient detection by growth cones.** *J Neurobiol* 1999, **41:**230-41.
11. Hentschel HG, van Ooyen A: **Models of axon guidance and bundling during development.** *Proc R Soc Lond B Biol Sci* 1999, **266:**2231-8.
12. Meinhardt H: **Orientation of chemotactic cells and growth cones: models and mechanisms.** *J Cell Sci* 1999, **112:**2867-74.
13. Richards LJ, Koester SE, Tuttle R, O'Leary DD: **Directed growth of early cortical axons is influenced by a chemoattractant released from an intermediate target.** *J Neurosci* 1997, **17:**2445-58.
14. Ren XC, Kim S, Fox E, Hedgecock EM, Wadsworth WG: **Role of netrin UNC-6 in patterning the longitudinal nerves of Caenorhabditis elegans.** *J Neurobiol* 1999, **39:**107-18.
15. Gomez TM, Spitzer NC: **Regulation of growth cone behavior by calcium: new dynamics to earlier perspectives.** *J Neurobiol* 2000, **44:**174-83.
16. Kim S, Ren XC, Fox E, Wadsworth WG: **SDQR migrations in Caenorhabditis elegans are controlled by multiple guidance cues and changing responses to netrin UNC-6.** *Development* 1999, **126:**3881-90.
17. Takei K, Chan TA, Wang FS, Deng H, Rutishauser U, Jay DG: **The neural cell adhesion molecules L1 and NCAM-180 act in different steps of neurite outgrowth.** *J Neurosci* 1999, **19:**9469-79.
18. Stein E, Tessier-Lavigne M: **Hierarchical organization of guidance receptors: silencing of netrin attraction by slit through a Robo/DCC receptor complex.** *Science* 2001, **291:**1928-38.
19. Thelen K, Kedar V, Panicker AK, Schmid RS, Midkiff BR, Maness PF: **The neural cell adhesion molecule L1 potentiates integrin-dependent cell migration to extracellular matrix proteins.** *J Neurosci* 2002, **22:**4918-31.
20. Yu TW, Bargmann CI: **Dynamic regulation of axon guidance.** *Nat Neurosci* 2001, **4 Suppl:**1169-76.
21. Godement P, Wang LC, Mason CA: **Retinal axon divergence in the optic chiasm: dynamics of growth cone behavior at the midline.** *J Neurosci* 1994, **14:**7024-39.
22. Mason CA, Wang LC: **Growth cone form is behavior-specific and, consequently, position-specific along the retinal axon pathway.** *J Neurosci* 1997, **17:**1086-100.
23. Mason C, Erskine L: **Growth cone form, behavior, and interactions in vivo: retinal axon pathfinding as a model.** *J Neurobiol* 2000, **44:**260-70.
24. Skaliora I, Adams R, Blakemore C: **Morphology and growth patterns of developing thalamocortical axons.** *J Neurosci* 2000, **20:**3650-62.
25. Oakley RA, Tosney KW: **Contact-mediated mechanisms of motor axon segmentation.** *J Neurosci* 1993, **13:**3773-92.
26. Fan J, Raper JA: **Localized collapsing cues can steer growth cones without inducing their full collapse.** *Neuron* 1995, **14:**263-74.
27. Goldberg DJ, Burmeister DW: **Stages in axon formation: observations of growth of Aplysia axons in culture using video-enhanced contrast-differential interference contrast microscopy.** *J Cell Biol* 1986, **103:**1921-31.
28. Danuser G, Oldenbourg R: **Probing f-actin flow by tracking shape fluctuations of radial bundles in lamellipodia of motile cells.** *Biophys J* 2000, **79:**191-201.
29. Katz MJ: **How straight do axons grow?** *J Neurosci* 1985, **5:**589-95.
30. Buettner HM: **Microcontrol of neuronal outgrowth.** In: *Nanofabrication and biosystems* Edited by: Hoch HC, Jelinski LW, Craighead HG. New York: Cambridge University Press; 1996:300-314.
31. Burt A: **An experimental and mathematical analysis of nerve growth cone motility based on cytoskeletal actin dynamics.** *PhD thesis* 2001 [http://wwwlib.umi.com/dissertations/dlnow/3026315]. Rutgers University, Chemical and Biochemical Engineering
32. Wang F-S, Liu C-W, Diefenbach TJ, Jay DG: **Modeling the role of myosin 1c in neuronal growth cone turning.** *Biophys J* 2003, **85:**3319-3328.
33. Moss F, McClintock PVE, eds: *Theory of continuous Fokker-Planck systems* First edition. Cambridge: Cambridge University Press; 1989.
34. Zheng JQ: **Turning of nerve growth cones induced by localized increases in intracellular calcium ions.** *Nature* 2000, **403:**89-93.
35. Zheng JQ, Wan JJ, Poo MM: **Essential role of filopodia in chemotropic turning of nerve growth cone induced by a glutamate gradient.** *J Neurosci* 1996, **16:**1140-9.
36. Forscher P, Smith SJ: **Actions of cytochalasins on the organization of actin filaments and microtubules in a neuronal growth cone.** *J Cell Biol* 1988, **107:**1505-1516.
37. Polinsky M, Balazovich K, Tosney KW: **Identification of an invariant response: stable contact with schwann cells induces veil extension in sensory growth cones.** *J Neurosci* 2000, **20:**1044-55.
38. Steketee MB, Tosney KW: **Contact with isolated sclerotome cells steers sensory growth cones by altering distinct elements of extension.** *J Neurosci* 1999, **19:**3495-506.
39. Tosney KW, Landmesser LT: **Growth cone morphology and trajectory in the lumbosacral region of the chick embryo.** *J Neurosci* 1985, **5:**2345-58.
40. Caudy M, Bentley D: **Pioneer growth cone morphologies reveal proximal increases in substrate affinity within leg segments of grasshopper embryos.** *J Neurosci* 1986, **6:**364-79.
41. Holt CE: **A single-cell analysis of early retinal ganglion cell differentiation in Xenopus: from soma to axon tip.** *J Neurosci* 1989, **9:**3123-45.
42. Halloran MC, Kalil K: **Dynamic behaviors of growth cones extending in the corpus callosum of living cortical brain slices observed with video microscopy.** *J Neurosci* 1994, **14:**2161-77.
43. Bovolenta P, Mason C: **Growth cone morphology varies with position in the developing mouse visual pathway from retina to first targets.** *J Neurosci* 1987, **7:**1447-60.
44. Yates PA, Roskies AL, McLaughlin T, O'Leary DD: **Topographic-specific axon branching controlled by ephrin-As is the critical event in retinotectal map development.** *J Neurosci* 2001, **21:**8548-63.
45. Fischer D, He Z, Benowitz LI: **Counteracting the Nogo receptor enhances optic nerve regeneration if retinal ganglion cells are in an active growth state.** *J Neurosci* 2004, **24:**1646-51.
46. Song HJ, Ming GL, Poo MM: **cAMP-induced switching in turning direction of nerve growth cones.** *Nature* 1997, **388:**275-9.
47. Goodhill GJ: **Mathematical guidance for axons.** *Trends Neurosci* 1998, **21:**226-31.
48. Cowan G, Pines D, Melnzer D, eds: *Complexity: Metaphors, models, and reality* Reading, MA: Addison Wesley Longman; 1994.
49. Bak P, Paczuski M: **Complexity, contingency, and criticality.** *Proceedings of the National Academy of Sciences of the United States of America* 1995, **92:**6689-6696.
50. Bak P: *How nature works: The science of self organized criticality* New York: Copernicus Springer-Verlag; 1996.
51. Ivins J, Raper J, Pittman R: **Intracellular calcium levels do not change during contact-mediated collapse of chick DRG growth cone structure.** *J Neurosci* 1991, **11:**1597-1608.

52. Tai HC, Buettner HM: **Neurite outgrowth and growth cone morphology on micropatterned surfaces.** *Biotechnol Prog* 1998, **14:**364-70.